Environmental Technology & Innovation 38 (2025) 104208

Contents lists available at ScienceDirect

Environmental Technology & Innovation

journal homepage: www.elsevier.com/locate/eti

Performance and microbial response of anaerobic membrane bioreactor to oil and salt co-occurrence in food wastewater treatment

Xueqi Chen [a], Ashley J. Ansari [b], Shuang Han [c], Yongzhen Peng [a], Xiaoye Song [a,*]

[a] National Engineering Laboratory for Advanced Municipal Wastewater Treatment and Reuse Technology, Engineering Research Centre of Beijing, Beijing University of Technology, Beijing 100124, China
[b] Centre for Technology in Water and Wastewater, School of Civil and Environmental Engineering, University of Technology Sydney, Ultimo, NSW 2007, Australia
[c] State Key Laboratory of Membrane Materials and Membrane Applications, Tianjin Motimo Membrane Technology Co.,Ltd., Tianjin 300457, China

ARTICLE INFO

Keywords:
Anaerobic membrane bioreactor
Salt
Oil
Methane production
Methanogenesis

ABSTRACT

High concentrations of oil and salt can adversely affect the effectiveness of anaerobic membrane bioreactors (AnMBRs) for food wastewater treatment, yet the impacts of their co-occurrence remain unknown. This study evaluated the performance of an AnMBR in response to simultaneous oil and salt stressors in synthetic food wastewater, in terms of methane production, membrane fouling, and microbial activity. Results show that either 8 g/L of cooking oil or 9 g/L NaCl in food wastewater caused the failure of AnMBR operation with a notable reduction in methane production and severe membrane fouling. However, the co-occurrence of oil and salt achieved a higher methane yield compared to oil stress alone. Additionally, the co-occurrence of oil and salt could alleviate osmotic stress to reduce microbial secretions and form macromolecular precipitates, thereby mitigating membrane fouling, compared to oil and salt alone. Such mitigation was due to the co-occurrence of high oil and salt to reduce long-chain fatty acids, enhancing living cells and their electron transfer activity. Further microbial analysis evidenced that the co-occurrence of oil and salt enriched hydrolytic and acidogenic bacteria (e.g. Bacteroidetes, Proteobacteria, Thermotogae, and Synergistetes) as well as hydrogenotrophic methanogens (e.g. *Methanolinea*) to upregulate genes related to methanogenesis for methane production. Furthermore, key enzymes involved in the hydrogenotrophic methanogenesis pathway (M00567) were augmented when 8 g/L of oil was simultaneously added with 9 g/L of salt.

1. Introduction

Food wastewater is an emerging issue for municipal waste treatment authorities due to the increasing production of food waste as a result of rapid urbanization. It has been reported that the concentration of salt (e.g., NaCl) in food wastewater is in the range of 7–12 g/L, whereas the oil concentration was more variable, ranging from 1.64 to 11.3 g/L (Dereli et al., 2015; Zhao et al., 2016). Moreover, some studies have found that the oil concentration is relatively high, generally above 6 g/L (Kurian et al., 2005). Anaerobic membrane

* Corresponding author.
E-mail address: songxiaoye@bjut.edu.cn (X. Song).

https://doi.org/10.1016/j.eti.2025.104208
Received 27 December 2024; Received in revised form 29 March 2025; Accepted 14 April 2025
Available online 15 April 2025

bioreactors (AnMBRs) present an innovative approach for both food wastewater treatment and resource recovery (Wang et al., 2023). During the anaerobic treatment of food wastewater, methane can be produced from organic materials like proteins and oils through the action of anaerobic microorganisms (Liu et al., 2024). Furthermore, the membrane in the AnMBR can decouple the sludge retention time (SRT) and hydraulic retention time (HRT) to improve organic methanization and effluent quality (Liu et al., 2020). However, the high oil and salt content, typical of food wastewater, can adversely affect the efficiency of AnMBR regarding methane production and membrane fouling (Ramos et al., 2014).

High oil concentrations can disrupt anaerobic microbial activity, leading to reduced methane production and severe membrane fouling in AnMBR systems. For instance, it has been reported that a high oil concentration of approximately 11.3 g/L reduced the methane yield by 25 % during AnMBR treatment of corn-to-ethanol wastewater (Dereli et al., 2014). Although oil has a high methane production potential (Deaver et al., 2021), its overdosage can lead to a substantial accumulation of volatile fatty acids (VFAs), which inhibit methanogen activity and therefore reduce methane production (Gao et al., 2024). More importantly, oil commonly hydrolyzes into long-chain fatty acids (LCFAs) (Palatsi et al., 2012), which are hydrophobic. These fatty acids create a physical barrier to inhibit the growth and activity of methanogenic bacteria by limiting the transfer of nutrients and metabolites (Zhang et al., 2023). Moreover, elevating oil concentrations can worsen membrane fouling. Han et al. (2024) observed that increasing the oleate-Na concentration from 2 to 4 g/L caused trans-membrane pressure (TMP) to rise from 0.19 to 0.21 kPa/d. This increase was attributed to the accumulation and subsequent adhesion of LCFAs onto polymeric membranes in AnMBR via hydrophobic interactions.

High salt concentration can also hinder the activity of anaerobic microbes (e.g. methanogens) and stimulate the production of soluble microbial production (SMP) and extracellular polymeric substance (EPS) (Xiao et al., 2022). These impacts could reduce methane production and aggravate membrane fouling (Kumar Biswal et al., 2020). Although Na^+ can enhance enzymatic activity and help maintain osmotic balance, its concentrations of exceeding 1 % can cause cell disintegration (Chen et al., 2008). Zhao et al. (2017) reported that increasing the salt concentration from 2 to 15 g/L caused an 88.5 % of reduction in methane yield. Such reduction was attributed to osmotic imbalance, which led to water loss from microbial cells and reduced enzyme activity, and eventually plasmolysis or cell death. Wang et al. (2023) also noted that increasing the salt concentration from 0 to 10 g/L increased the membrane fouling rate up to 24.4 kPa/d given the excessive secretion of SMP at high salinity. Furthermore, elevated salt levels can disrupt the multivalent cation bridge between EPS molecules, causing sludge deflocculation and deterioration to aggravate membrane fouling (De Temmerman et al., 2014).

Despite recent studies to examine AnMBR performance in response to the individual occurrence of salt or oil, the interactive impacts of these two inhibitors remain unknown. Therefore, this research sought to explore the impacts of high oil and salt co-occurrence on AnMBR performance during food wastewater treatment. Cooking oil and NaCl were incorporated into synthetic food wastewater to reach the inhibitory levels. AnMBR performance was evaluated by monitoring methane yield, membrane fouling, and VFAs production in a lab-scale reactor. To further understand the microbial activity, living cell counts and electron transfer system (ETS) activity were analyzed. Furthermore, the dynamics of microbial community structure and metabolic functions within the mixed liquor and membrane surface were analyzed to elucidate the mechanisms driving AnMBRs response to the co-occurrence of oil and salt.

2. Materials and methods

2.1. Influent composition and sludge inoculum

The chemical oxygen demand (COD) of food wastewater has been reported to the range from 500 to 10,000 mg/L with most values approaching 5000 mg/L (He et al., 2023, 2005). The COD of 5000 mg/L was selected for the synthetic food wastewater in this study.

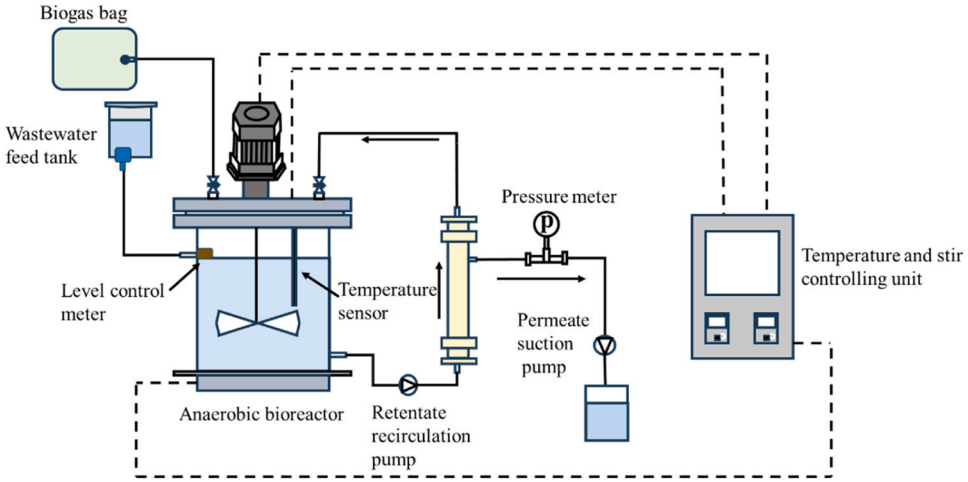

Fig. 1. Schematic representation of the lab-scale AnMBR system.

The wastewater was prepared daily and consisted of glucose (5000 mg/L), urea (540 mg/L), and potassium dihydrogen phosphate (220 mg/L). The trace elements, including 100 mg/L $MgCl_2{\cdot}6\,H_2O$, 50 mg/L $CaCl_2$, 310 mg/L NaCl, 5 mg/L $CoCl_2{\cdot}6\,H_2O$, 25 mg/L $FeCl_2$, and 5 mg/L $NiCl_2{\cdot}6\,H_2O$ (Jeong et al., 2017), were also added. The high salt and oil content of real food wastewater was simulated using NaCl and blended oils from Dragonfish (containing 55 % peanut oil, 22 % sunflower oil, 12 % linseed oil, 6 % soybean oil, and 5 % canola oil).

The seed sludge utilized in the AnMBR was sourced from a municipal treatment plant in Beijing, China. The sludge underwent acclimatization for more than 60 days to enhance its performance in anaerobic digestion, achieving stable removal of organic matter exceeding 90 %, with methane content in the biogas reaching above 60 %.

2.2. AnMBR configuration and operation

This study utilized a lab-scale AnMBR system (Fig. 1). An external membrane cell, constructed from stainless steel, was included in the AnMBR and housed a tubular ceramic microfiltration membrane (MF) (Bona Biotechnology, China) with a pore size of 0.45 μm and an effective filtration area of 0.08 m^2. The AnMBR also included a continuous stirred tank reactor with a working volume of 4.4 L, equipped with a water bath to maintain the operating temperature at 35 ± 1 °C. A biogas analyzer (Biogas 5000, Geotech, UK) was used to analyze the composition of the biogas collected from the gas bag connected to the AnMBR. A high-precision pressure sensor (HG-808XB, Ho Asia, China; ± 0.1 kPa) monitored the TMP. The mixed liquor in the bioreactor was pumped into the MF membrane unit using a peristaltic pump (BT600FC, China), while a separate peristaltic pump (BT600FC, China) drew permeate from the MF membrane, operating on a cycle of 11 minutes on and 1 minute off.

Batch experiments were conducted to assess the effects of variable salt and oil concentrations on the anaerobic digestion of food wastewater (Text 1, Supplementary Information). In brief, the results demonstrated that while individual additions of oil (8.0 and 10.0 g/L) and salt (9.0 and 12.0 g/L) inhibited methanogenesis, their co-occurrence at 8 g/L oil and 9 g/L salt enhanced methane yield by up to 30.45 % compared to individual additions. However, higher concentrations (O8S12, O10S9, and O10S12) resulted in severe acid accumulation and significant methanogenic inhibition, indicating that 8 g/L oil and 9 g/L salt represent the threshold of inhibition. Based on these findings, four treatments were designed for continuous AnMBR operation to assess its response to the inhibitory effects of simultaneous oil and salt. They included adding oil and salt to the feed solution at 0 and 0 g/L, 8 and 0 g/L, 0 and 9 g/L, 8 and 9 g/L, and denoted as O0S0, O8S0, O0S9, and O8S9, respectively. All treatments were continuously operated for 25 days or until significant AnMBR collapse due to high oil and salt inhibition occurred. The AnMBR system was operated at the initial mixed liquor suspended solids (MLSS) content of 10 g/L and HRT of 2 days. No sludge was discharged except for sampling purposes. Sodium bicarbonate was used periodically to regulate the mixed liquor pH at 7.0 ± 0.1.

2.3. Sampling and analytical methods

2.3.1. Basic water quality parameters

Influent, mixed liquor, and effluent samples were periodically collected for water quality analysis. All liquid samples were processed for the measurement of pH and electrical conductivity using a pH/conductivity meter (ST3100 M, OHAUS, USA), COD using the standard dichromate method, VFAs using gas chromatograph (GC7890, Agilent, USA) (Li et al., 2017), and LCFAs using a gas chromatography-mass spectrometry (Agilent Technologies Inc. CA, UAS) (Li et al., 2015).

2.3.2. Sludge characteristics

Mixed liquor samples were also prepared for sludge characterization. The concentration of EPS and SMP were assessed by quantifying their polysaccharide and protein contents (Liu et al., 2022). The Lowry-Folin method was used to quantify protein content, and the phenol-sulfuric acid method was employed to measure polysaccharide content (Miao et al., 2018). The particle size distribution of the mixed liquor was analyzed by a laser particle size analyzer (Microtrac, USA, S3500).

The ETS activity of microbial communities was measured using the INT 2-(p-iodophenyl)-3-(p-nitrophenyl)-5-phenyltetrazolium chloride method (Tian et al., 2017). The percentage of living cells was measured by flow cytometry (Luminex, America). All samples for the analysis of cell viability were prepared following established procedures (Brown et al., 2015), and then stained with SYTO9 (Invitrogen, America) and PI (Solarbio, China) before being incubated in the dark for 15 minutes at room temperature (Benito et al., 2020). After incubation, a flow cytometer was used to analyze fluorescence patterns, enabling the differentiation of live and dead cells based on their fluorescence intensities.

2.3.3. Membrane fouling characterization

TMP was measured in this study to assess membrane fouling. Furthermore, the Darcy law was used to determine the distribution of membrane resistance (Ninomiya et al., 2020; Wang et al., 2022):

$$R_t = \frac{TMP}{\mu J}\# \tag{1}$$

$$R_t = R_m + R_c + R_f\# \tag{2}$$

where J represents the permeate flux ($m^3{\cdot}m^{-2}{\cdot}s^{-1}$); μ denotes the viscosity of the permeate (Pa·s); R_t, R_m, R_c and R_f represent the total

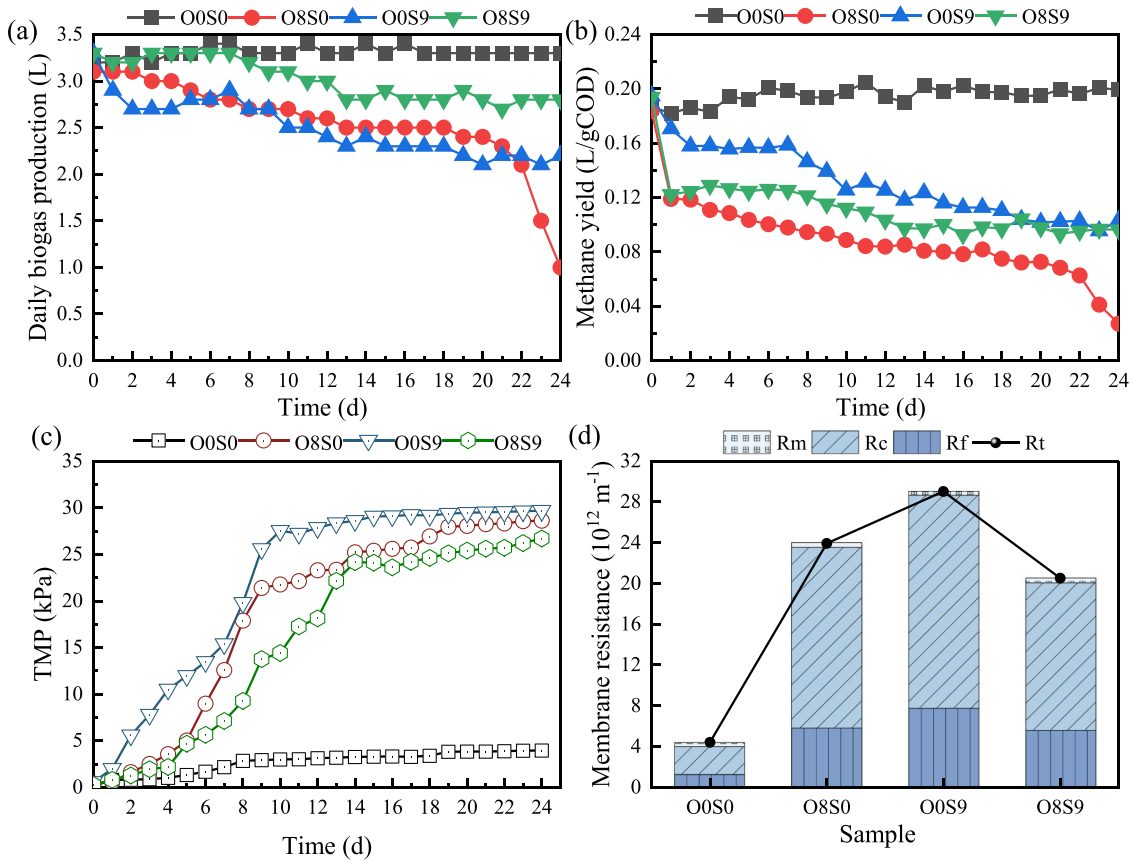

Fig. 2. Effects of high oil and salt concentrations on (a) biogas production, (b) methane yield, (c) TMP and (d) distribution of membrane resistance in AnMBR operation. The experiments were conducted under four distinct conditions, with varying oil (O) and salt (S) concentrations in the feed solution: O0S0 (0 g/L oil, 0 g/L salt), O8S0 (8 g/L oil, 0 g/L salt), O0S9 (0 g/L oil, 9 g/L salt), and O8S9 (8 g/L oil, 9 g/L salt).

resistance (m^{-1}), intrinsic membrane resistance (m^{-1}), the cake layer resistance (m^{-1}) and the fouling blocking resistance (m^{-1}), respectively.

2.3.4. Microbial community analysis

At the conclusion of the AnMBR operation, the mixed liquor and cake layer were collected for high-throughput sequencing to analyze the microbial community structure. The V3–V4 hypervariable region of bacteria 16 S rRNA gene was amplified using the universal primer 341 F (5'-CCTAYGGGRBGCASCAG-3') and 806 R (5'-GGACTACNNGGGTATCTAAT-3'). For the amplification of the V3–V4 hypervariable region of the archaeal 16S rRNA gene, the primers 519 F (5'-CAGCCGCCGCGGTAA-3') and 915 R (5'-GTGCTCCCCCGCCAATTCCT-3') were used. The amplification products were purified and then sequenced using NovaSeq 6000 (Illumina, United States).

2.3.5. Data analysis

FlowJo software was used to process the cell viability data and differentiate live and dead cells. The functional gene analysis was conducted using the Kyoto Encyclopedia of Genes and Genomes Orthology (http://www.kegg.jp/kegg/ko.html). Microsoft Excel 2019 was used for statistical analysis. The graphical representations were generated via Origin 2022.

3. Results and discussion

3.1. Methane production and membrane fouling

High oil and high salt concentrations in food wastewater, when tested separately, each resulted in a notable decline in methane production, ultimately causing AnMBR system failure (Fig. 2a&b). When no oil or salt was added (i.e. O0S0), this treatment exhibited stable daily biogas production of approximately 3.3 ± 0.1 L/d and a methane yield of approximately 0.20 L/gCOD. In practice, methane was partially dissolved in wastewater, leading to actual methane yield that was lower than theoretical values (Li et al., 2023). By contrast, the daily biogas production and methane yield gradually declined to 1.0 L/d and 0.03 L/gCOD on day 22, respectively, for the O8S0 treatment. This finding could be related to the conversion of high oil concentration (8 g/L) into LCFAs, which strongly adhere to the sludge, resulting in sludge flotation during AnMBR operation (Holohan et al., 2022; Szabo-Corbacho et al., 2024). It has been reported that oil could be hydrolyzed to LCFAs and glycerol to damage microbial activity and growth, thereby leading to the failure of anaerobic digestion (Rasit et al., 2015). Moreover, the O0S9 treatment experienced a significant decline in biogas production and methane yield to 2.2 L/d and 0.10 L/gCOD, respectively. Similar findings have been extensively documented, as high salt content can osmotically impair the activity of key enzymes (e.g. dehydrogenase) and cells (Buenaño-Vargas et al., 2024). Anwar et al. (2016) investigated the effects of different salt concentrations on the long-term anaerobic digestion of real food waste and found that at 16 g/L NaCl, the methane yield was reduced by 80.6 % compared to the group without salt addition.

Compared to the O8S0 treatment, the O8S9 treatment suffered fewer negative impacts from the high oil concentrations. This result could be attributed to the adsorption and encapsulation of Na^+ by oil and its derivations (e.g. LCFAs) to mitigate their inhibitory effects on microbes when oil and salt co-occurred (Liu and Jiang, 2020). However, the methane yield in O8S9 was lower than that in O0S9, possibly due to LCFAs from oil hydrolysis to adsorb onto cell surfaces and hinder nutrient and electron transfer (Elsamadony et al., 2021). This interference negatively impacted methane production, resulting in a lower methane yield. Li et al. (2023) observed that the presence of oil at 5 g/L and salt at 6 g/L significantly reduced methane production which was further aggravated as their concentrations increased to 25 and 12 g/L, respectively.

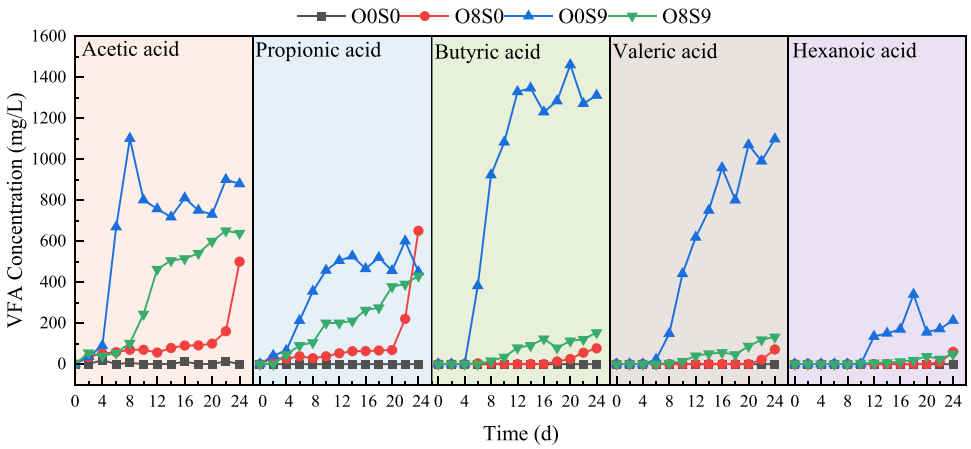

Fig. 3. Effects of high oil and salt contents on volatile fatty acids production. The experiments were conducted under four distinct conditions, with varying oil (O) and salt (S) concentrations in the feed solution: O0S0 (0 g/L oil, 0 g/L salt), O8S0 (8 g/L oil, 0 g/L salt), O0S9 (0 g/L oil, 9 g/L salt), and O8S9 (8 g/L oil, 9 g/L salt).

Membrane fouling was characterized by TMP variation and membrane resistance, which varied in response to the addition of oil and salt (Fig. 2c&d). In the O0S0 treatment, membrane fouling was negligible as evidenced by an insignificant increase in TMP by the end of the experiment and a low R_t value. By contrast, when 8 g/L of oil was added to the influent, a notable TMP increase to 28.61 kPa was observed by the conclusion of the AnMBR operation, with a daily increase of 1.15 kPa. Ramos et al. (2014) also reported a notable increase in membrane fouling rate from 0.09 to 3.95 mbar/d as the oil concentration rose from 0.5 to 6.0 g/L. Further analysis of the membrane resistance distribution in the O8S0 treatment showed that R_c was the main component of R_t (accounting for 74.00 %) (Fig. 2d), possibly due to the high oil content which induced pore blockage and the formation of a cake layer as the main mechanisms of membrane fouling (Chung et al., 2023). A similar degree of aggravated membrane fouling also occurred in the O0S9 treatment, whereby the TMP increased to 29.68 kPa with the daily rate of 1.19 kPa/d. This notable TMP increase could be related to the increased SMP and EPS production (up to 16.28 and 34.33 mg/gVSS, respectively as shown in Fig. S3) from microbial activity and growth in response to the high salinity (Wang et al., 2023). The membrane resistance analysis showed that the O0S9 treatment had the highest value of R_c (2.09×10^{13} m^{-1}), indicating the key role of cake layer formation to membrane fouling. Indeed, high salt content reduced the sludge particle size (Table S3) to accelerate biomass movement and then attachment onto the membrane surface (Lin et al., 2009). Compared to O8S0 and O0S9, the O8S9 treatment with oil and salt co-occurrence alleviated membrane fouling with the TMP increase at 1.07 kPa/d to 26.8 kPa by the end of AnMBR operation. Such alleviation could be related to the formation of macromolecular precipitates from Na^+ ions and LCFAs to enlarge sludge particle size and thus reduce their deposition on the membrane surface (Dereli et al., 2014). Moreover, the adherence of LCFAs to the surface of microbes reduced the osmotic stress from high salinity (9 g/L), to mitigate SMP secretion (9.57 mg/g VSS) and thus membrane fouling (Liu et al., 2017a).

3.2. LCFAs and VFAs production

It has been widely reported that LCFAs from oil hydrolysis could impair microbes, particularly acetoclastic and hydrogenotrophic methanogens in anaerobic digestion (Lalman and Bagley, 2001). At the end of the AnMBR operation, the total content of LCFAs in the O8S9 treatment (330.60 mg/L) was 20.86 % lower than that in the O8S0 treatment (417.73 mg/L) (Table S2). Such lower production of LCFAs was possibly due to the binding of Na^+ to LCFAs, which could alleviate the inhibitory effects of LCFAs and thereby promote their further conversion (Liu and Jiang, 2020).

Compared to the O0S0 treatment, significant accumulation of VFAs were observed in the O8S0, O0S9, and O8S9 by the conclusion of the AnMBR operation (Fig. 3). In the O8S0 treatment, significant VFA accumulation occurred from day 20 up to 1358.89 mg/L with acetic acid and propionic acid concentrations at 500.17 mg/L and 650.52 mg/L, respectively (Fig. 3). Such notable VFA accumulation inhibited microbial activity, leading to system failure (Long et al., 2012). Xiao et al. (2017) found that when treating real food

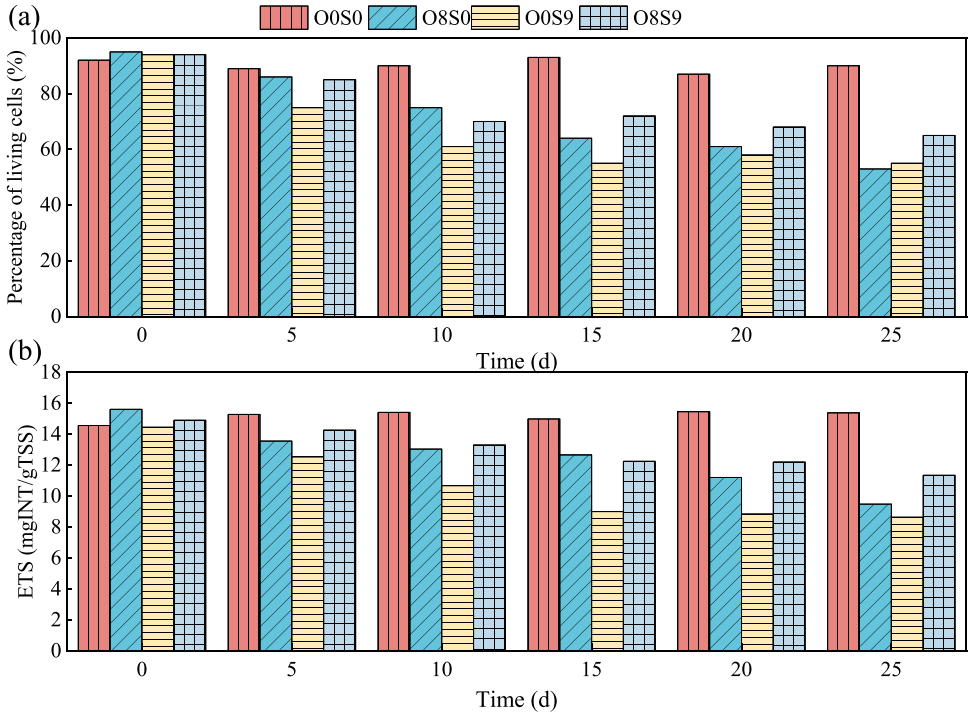

Fig. 4. Effects of high oil and salt contents on (a) percentage of living cells and (b) electron transport system (ETS) activity in AnMBR operation. The experiments were conducted under four distinct conditions, with varying oil (O) and salt (S) concentrations in the feed solution: O0S0 (0 g/L oil, 0 g/L salt), O8S0 (8 g/L oil, 0 g/L salt), O0S9 (0 g/L oil, 9 g/L salt), and O8S9 (8 g/L oil, 9 g/L salt).

wastewater with a pilot-scale AnMBR (oil concentration from 4.4 to 6.3 g/L), maintaining an appropriate OLR (4.7 kg COD/m^3) was crucial for ensuring stable system performance, including VFA accumulation and pH stability. Similar VFA accumulation to 3753.23 mg/L also occurred to the O0S9 treatment with the concentration of butyric acid and valeric acid to 1311.17 mg/L and 1099.07 mg/L by the conclusion of the AnMBR operation, respectively (Fig. 3), which was due to the salt inhibited the methanogens activity which impede the conversion of VFAs into biogas (Martinez-Quintela et al., 2024). Compared to the O0S0 treatment, the O8S9 treatment exhibited relatively higher VFA concentrations, however was much lower than that in the O0S9 treatment with the total concentration of less than 1500 mg/L. This reduction could be attributed to LCFAs from oil hydrolysis as an osmotic pressure buffer to facilitate VFA utilization by methanogenesis. Similar results have also been reported by Liu et al. (2017b) who observed an increase in oil concentration from 5 to 35 g/L reduce VFA production by approximately 30 % at the salt of 6 g/L. Nevertheless, compared to O8S0, the O8S9 treatment exhibited a higher concentration of VFAs, possibly due to the addition of salts to facilitate the conversion of LCFAs to VFAs (Liu and Jiang, 2020).

3.3. Living cells and electron transport system activity

The percentage of living cells was stable at 90.17 % for the O0S0 treatment, which however, decreased to 53 % and 55 % in the O8S0 and O0S9 treatments (Fig. 4a). Compared to O8S0 and O0S9, the percentage of living cells in the O8S9 treatment increased by 22.64 % and 18.18 %, respectively. These results provided direct evidence of the suppressive effects of high salt and oil concentrations on microbial growth during AnMBR operation, which could be alleviated to some extent by their co-occurrence. Such conclusion could be further confirmed by ETS analyses. Compared to a stable ETS of 15.18 $\pm$ 0.31 mg INT/gTSS in O0S0, ETS decreased notably in the O8S0 and O0S9 treatments, but recovered for the O8S9 treatment (Fig. 4b).

3.4. Microbial dynamics

3.4.1. Microbial community structure in the bioreactor

Despite the addition of varying amounts of oil and salt in the synthetic wastewater, the predominant bacterial communities at the phylum level were comparable across the four AnMBR systems (Fig. 5a). They included Bacteroidetes, Proteobacteria, Thermotogae and Synergistetes. Nevertheless, the high salt and oil concentrations resulted in a significant difference in their relative abundances in AnMBR operation.

Bacteroidetes comprised 18.03 % in the O0S0 treatment, but this decreased to 11.90 % and 15.17 % in the O8S0 and O0S9 treatments, respectively, due to the inhibitory effects of oil and salt. By contrast, Bacteroidetes constituted 22.02 % of the community

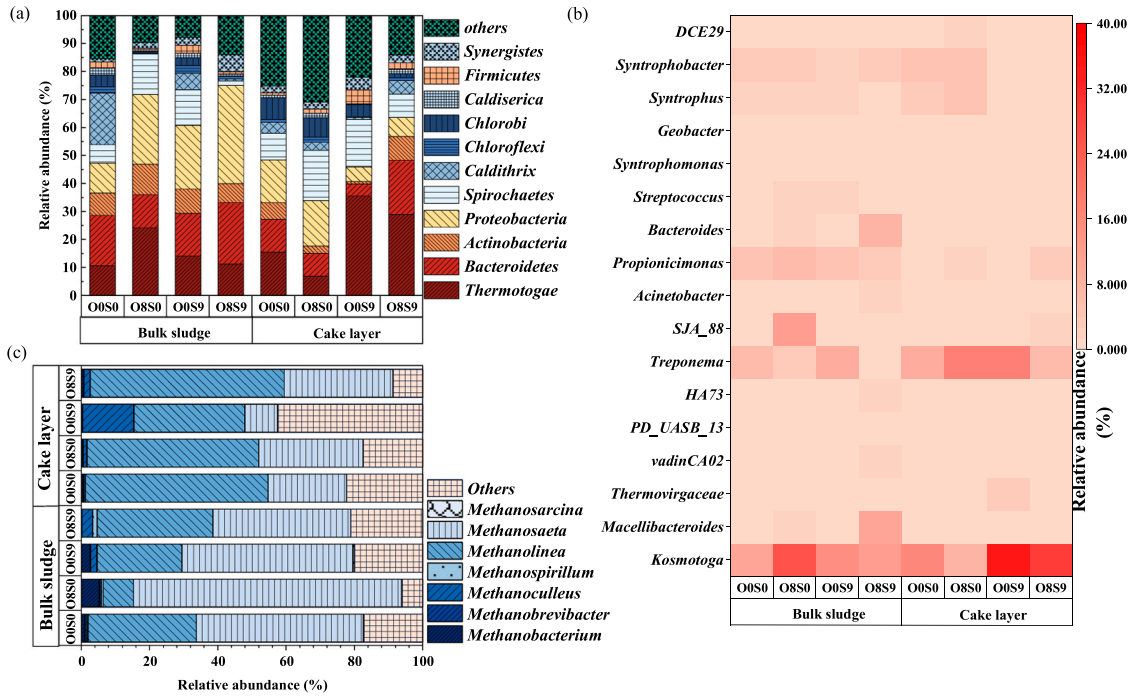

Fig. 5. Microbial community structure in the bioreactor and the membrane cake layer: (a) bacteria community at the phylum level; (b) bacteria community at the genus level; and (c) archaeal community at the genus level. The experiments were conducted under four distinct conditions, with varying oil (O) and salt (S) concentrations in the feed solution: O0S0 (0 g/L oil, 0 g/L salt), O8S0 (8 g/L oil, 0 g/L salt), O0S9 (0 g/L oil, 9 g/L salt), and O8S9 (8 g/L oil, 9 g/L salt).

in the O8S9 treatment. This phylum has been reported as a main hydrolytic bacterium in acidogenesis to convert organics into VFAs (Ma et al., 2021; Xu et al., 2021). As such, the enhanced COD removal rate observed in the O8S9 treatment could be attributed to its higher relative abundance of Bacteroidetes (Fig. S2). At the genus level, *Macellibacteroides*, reported to participate in VFAs generation, played a key role in influencing the abundance of Bacteroidetes (Luo et al., 2021). Its relative abundance in the O8S9 treatment (10.42 %) exceeded that in other treatments, potentially explaining the higher concentrations of acetic and butyric acids in this group.

The relative abundance of Proteobacteria was highest in the O8S9 treatment at 35.05 % (Fig. 5a), which indicated that the presence of both oil and salt favored Proteobacteria enrichment. Chen et al. (2019) attributed this to their strong salinity tolerance, enabled by ion regulation mechanisms that balance osmotic pressure through K^+ import and Na^+ export. Moreover, soybean oil has been shown to promote Proteobacteria growth due to their role in LCFA degradation (Sun et al., 2023). Oil and salt co-occurrence provided rich carbon and created favorable metabolic environments for hydrolysis and acidification to produce acetic acid during anaerobic digestion (Wu et al., 2017). Indeed, the predominance of the phylum Proteobacteria was primarily due to the genus *Syntrophobacter*, which were able to resist the high oil conditions due to their active role in the anaerobic methanization of LCFAs (Holohan et al., 2022; Putra et al., 2020), facilitating their further conversion. As a result, the improved performance of the O8S9 treatment could be linked to the higher relative abundance of *Syntrophobacter* compared to the O8S0 treatment (Fig. 5b).

The high oil and salt content in the O8S9 treatment increased the relative abundance of Synergistetes to 6.10 %, enabling efficient biodegradation of complex organic matter and fermentation of acetic acid into H_2 and CO_2 (Jang et al., 2014). In contrast, this abundance was only 1.09 %, 2.07 %, and 2.83 % in the O0S0, O8S0, and O0S9, respectively (Fig. 5a). Furthermore, a higher relative abundance of *HA73* and *vadinCA02*, both from the phylum Synergistetes, was observed in the O8S9 treatment (Fig. 5b). The co-occurrence of oil and salt could enrich Synergistetes, particularly *HA73* and *vadinCA02*, which play key roles in protein biodegradation, acetic acid production, and the acceleration of hydrolysis and acidification processes (Yin et al., 2017). These functions likely contributed to the improved COD removal rate observed in the O8S9 treatment (Fig. S2).

Compared to the O0S0 treatment, oil and salt addition enhanced the relative abundance of Thermotogae in the O8S0, O0S9, and O8S9 treatments (Fig. 5a). Studies have indicated that Thermotogae could tolerate elevated LCFAs by converting glycerol into acetate and hydrogen (Jensen et al., 2014) and adapt to high-salinity conditions (García Rea et al., 2023). Nevertheless, the co-occurrence of oil and salt in the O8S9 treatment reduced the enrichment of Thermotogae in comparison with the O8S0 and O0S9 treatments, which could be attributed to the intolerance to the combined stress induced by the co-occurrence of oil and salt. At the genus level, the key genus determining the phylum Thermotogae was *Kosmotoga*, which was involved in the metabolism of acetic acid and propionic acid (Yin et al., 2017). The relative abundance of *Kosmotoga* was 24.01 %, 14.13 %, 11.22 %, and 10.63 % in the O8S0, O0S9, O8S9, and O0S0 treatments, respectively (Fig. 5b). The higher abundance of *Kosmotoga* was likely due to the increased levels of acetic acid and propionic acid caused by the addition of oil and salt. These metabolites provide a favorable substrate for *Kosmotoga*, enhancing their growth and metabolic activity (Okoro et al., 2016).

The archaea community was predominantly composed of *Methanosaeta* and *Methanolinea* at the genus level (Fig. 5c). *Methanosaeta*, an acetoclastic methanogen (Cai et al., 2021), constituted 48.79 % of the community in the O0S0 treatment, increasing to 78.44 % in the O8S0 treatment and 50.02 % in the O0S9 treatment. By contrast, this relative abundance decreased to 40.19 % in the O8S9 treatment. In contrast, the relative abundance of *Methanolinea*, a strictly hydrogenotrophic methanogen that reduced CO_2 into CH_4 using H_2 as an electron donor (Fujihira et al., 2018), increased from 8.83 % in the O8S0 treatment and 24.72 % in the O0S9 treatment

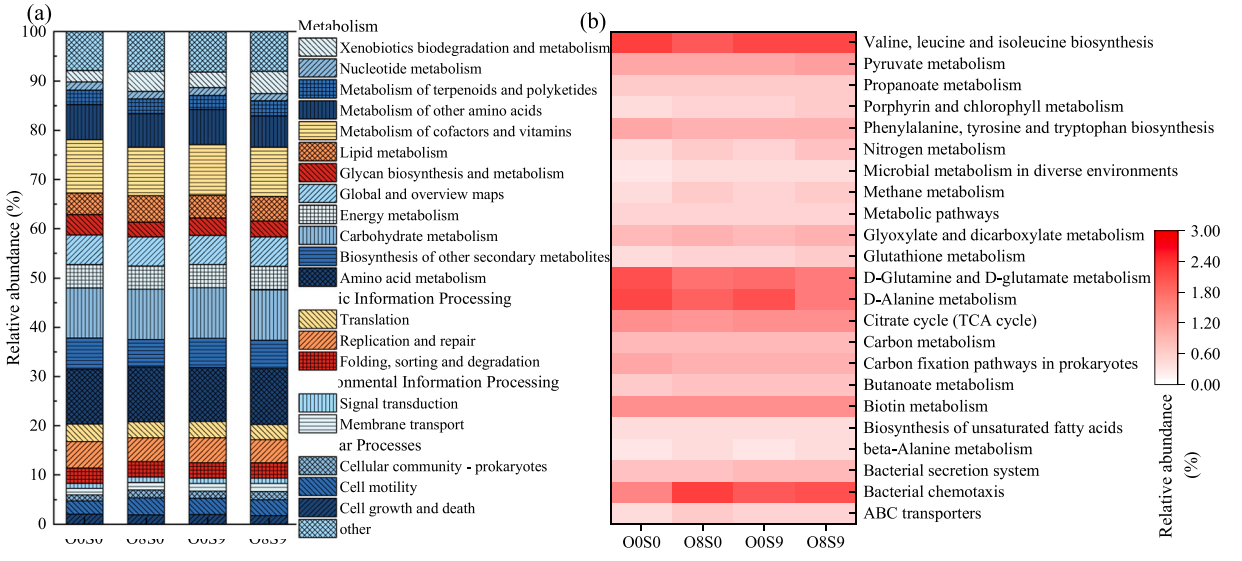

Fig. 6. Microbial metabolism function profiles of each group at (a) KEGG level II and (b) KEGG level III in AnMBR operation. The experiments were conducted under four distinct conditions, with varying oil (O) and salt (S) concentrations in the feed solution: O0S0 (0 g/L oil, 0 g/L salt), O8S0 (8 g/L oil, 0 g/L salt), O0S9 (0 g/L oil, 9 g/L salt), and O8S9 (8 g/L oil, 9 g/L salt).

to 33.77 % in the O8S9 treatment. These findings suggested that the co-occurrence of high concentrations of oil and salt could impede the growth of acetoclastic methanogens while selectively enhancing the accumulation of specific hydrogenotrophic methanogens (Evans et al., 2019).

3.4.2. Microbial community structure in the membrane cake layer

To gain deeper insights into the relationship between membrane fouling and the high concentrations of oil and salt, the microbial community of the foulant cake layer was assessed (Fig. 5a&b). The main microbes in the membrane cake layer included Bacteroidetes (4.32–19.35 %) and Proteobacteria (6.81–16.23 %). Bacteroidetes, as a carbohydrate degrader, could produce EPS to induce membrane fouling (Niu et al., 2021). Proteobacteria, as the predominant phylum associated with membrane fouling, could secrete EPS and further promote the cake layer formation (Lei et al., 2021).

Bacteroidetes constituted 11.80 % in the O0S0 treatment, which decreased to 8.11 % and 4.32 % in the O8S0 and O0S9 treatments, respectively, but increased to 19.35 % in the O8S9 treatment. This profile was consistent with that occurred in the bioreactor, possibly due to microbes in the bioreactor were dragged by the permeate flow and adhered on the membrane surface or cake sludge (Hong et al., 2019). It was noteworthy that Bacteroidetes could degrade carbohydrates and proteins in the cake layer (Meng and He, 2015), thereby mitigating membrane fouling in the O8S9 treatment in comparison to O8S0 and O0S9 treatments.

The relative abundance of Proteobacteria increased from 15.18 % in the O0S0 treatment to 16.23 % in the O8S0 treatment, while it decreased to 5.19 % and 6.81 % in the O0S9 and O8S9 treatments, respectively. This was probably due to the availability of LCFAs provided by the added oil, which serves as a rich carbon source, facilitating the proliferation and metabolic activity of Proteobacteria. In contrast, the increased salinity probably introduced nutritional competition or inhibitory effects that suppressed the relative abundance of Proteobacteria in the cake layer. *Syntrophobacter*, a genus within the Proteobacteria phylum, was recognized as one of the primary pioneers in biofilm formation (Lei et al., 2021). The relative abundance of *Syntrophobacter* increased from 1.73 % in the O0S0 treatment to 1.77 % in the O8S0 treatment, respectively. *Syntrophobacter* has been identified as a contributor to the conversion of propionic acid (Cao et al., 2021), suggesting that higher levels of propionic acid in the O8S0 treatment would support the proliferation of *Syntrophobacter*, thereby enhancing its role in propionic acid degradation. However, their relative abundances dropped significantly to 0.38 % and 0.41 % in the O0S9 and O8S9 treatment, respectively. This decline could be attributed to the moderate salt tolerance of *Syntrophobacter* (max 1.2 M Na^{+}) (Sorokin and Chernyh, 2016), which suggested that high concentrations of salt (9 g/L) impacted the growth of this genus. The relatively low abundance of *Syntrophobacter* in the O8S9 treatment was detrimental to biofilm formation, thereby effectively mitigating the potential for membrane fouling.

3.5. Microbial metabolic functions in the bioreactor

To thoroughly understand the impact of oil and salt on microbial metabolic functions, a pairwise comparison based on functional differences in the KEGG was conducted. The secondary metabolic pathways (level II) mainly included carbohydrate metabolism (10.21 %-10.30 %), metabolism of cofactors and vitamins (9.82 %-10.83 %), and amino acid metabolism (11.00 %-11.34 %) (Fig. 6a). Compared to the O8S0 and O0S9 treatment, the co-occurrence of high oil and salt content in the O8S9 treatment promoted amino acid metabolism, accounting for 11.34 % of the metabolic group. This enhancement increased amino acid transport and metabolism, accelerating the metabolism of protein-like organic substance to facilitate the biodegradation of macromolecular organics (Zhang et al., 2023).

The KEGG level III analysis was performed to clarify the specific metabolic pathways and functional genes involved in the anaerobic digestion process (Fig. 6b). Pyruvate metabolism was related to hydrolysis, which could facilitate the conversion of pyruvate to acetyl-CoA and its abundance indicated the intensity of hydrolysis (Chen et al., 2024; Wu et al., 2023). The increased abundance of pyruvate

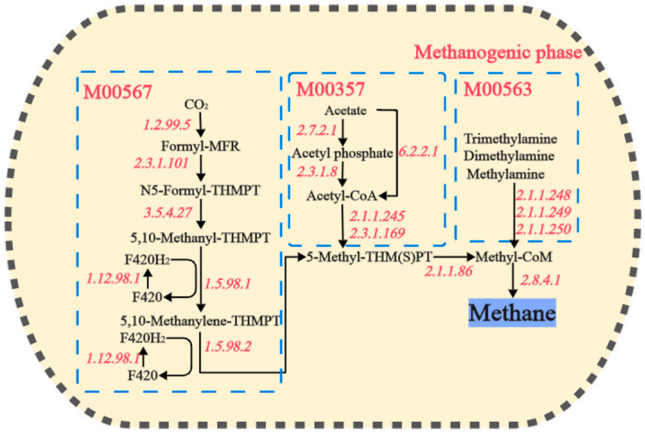

Fig. 7. Key metabolic pathways and associated genes encoding functional enzymes involved in methanogenesis during the operation of AnMBR under different oil and salt conditions.

metabolism in O8S9 was mainly due to its high activity of key enzymes (e.g. NAD-dependent lactate dehydrogenase) in propionate formation. This result suggested that oil and salt co-occurrence promoted hydrolysis and thus enhanced propionic acid production (Fig. 3). The TCA cycle served as the final metabolic pathway for the three major nutrients (carbohydrates, lipids, and amino acids), which were essential for energy metabolism (Wang et al., 2023). The proportion of the TCA cycle in the O8S9 treatment slightly increased by 6.16 % and 1.10 % in comparison to O8S0 and O0S9, respectively, thereby enhancing the microbial activity and organic metabolism (Wang et al., 2023).

3.6. Methanogenic pathway

To investigate the methane metabolism, genes for key enzymes in three methanogenic pathways were analyzed: hydrogenotrophic (M00567), acetoclastic (M00357), and methylotrophic (M00563) (Fig. 7). These pathways played crucial roles in methane production, with the M00357 being the primary contributor (43.7 %-51.1 %), followed by the M00567 (16.9 %-47.8 %).

In M00567, methane was produced by CO_2 and H_2, with coenzyme F420 acting as a redox cofactor (Gao et al., 2024). Methylenetetrahy-dromethanopterin dehydrogenase [EC:1.5.98.1], 5,10-methyl-enetetrahydromethanopterin reductase [EC:1.5.98.2] and coenzyme F420 hydrogenase [EC:1.12.98.1] were the primary enzymes involved in the production of coenzyme F420. Gu et al. (2024) reported that coenzyme F420 was the key enzyme unique to methanogenic bacteria, serving a critical function in methane production. Consequently, the higher relative abundance of relevant enzymes in the O8S9 treatment (Fig. 8a) suggested that the co-occurrence of high content oil and salt enhanced the hydrogenotrophic methanogenesis pathway (M00567), which was aligning with the elevated levels of hydrogenotrophic methanogens discussed in Section 3.4.

Key enzymes associated with the M00357 pathway included acetate kinase [EC:2.7.2.1], phosphate acetyltransferase [EC:2.3.1.8], and acetyl-CoA synthetases [EC:6.2.1.1]. Notably, acetyl-CoA synthetase played a central role in acetoclastic methanogenesis, facilitating the conversion between acetate and acetyl-CoA (Dang et al., 2023), a critical intermediate in methane biosynthesis. The elevated relative abundance of [EC:6.2.1.1] observed in the O8S9 treatment suggested an enhanced availability of substrates for the methanogenic process, which likely contributed to the increased methane yield under this condition compared to the condition with oil addition alone (Fig. 8b).

Enzymes involved in M00563 primarily converted methanol and trimethylamine / dimethylamine / methylamine to methane (Yun et al., 2023). And the M00563 accounted for relatively little part of the overall methane production (Fig. 8c). In contrast to the O8S0 and O0S9 treatments, where oil and salt were present individually, the abundance of genes encoding functional enzymes in the O8S9 treatment was lower, suggesting that the co-occurrence of oil and salt might inhibit the expression of genes associated with the M00563.

4. Conclusion

The results demonstrate that the high oil and salt concentrations of food wastewater could alleviate their individual inhibition to mitigate membrane fouling in AnMBR operation by boosting the conversion of LCFAs to VFAs and forming macromolecular precipitates, which effectively diminished the concentrations of SMP as well as restrained their deposition on the membrane surface,

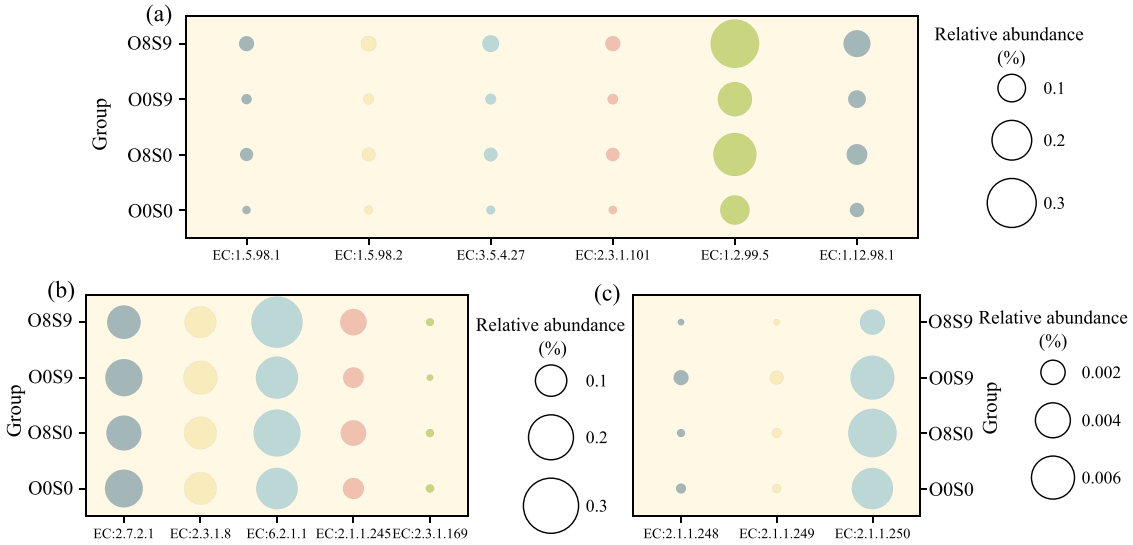

Fig. 8. Relevant abundance of functional enzyme-encoding genes involved in methanogenesis in AnMBR operation: (a) hydrogenotrophic methanogenesis pathway (M00567); (b) acetoclastic methanogenesis pathway (M00357); and (c) methylotrophic methanogenesis pathway (M00563). The experiments were conducted under four distinct conditions, with varying oil (O) and salt (S) concentrations in the feed solution: O0S0 (0 g/L oil, 0 g/L salt), O8S0 (8 g/L oil, 0 g/L salt), O0S9 (0 g/L oil, 9 g/L salt), and O8S9 (8 g/L oil, 9 g/L salt).

consequently alleviating membrane fouling. Moreover, compared to oil addition alone, the co-occurrence of oil and salt achieved a higher methane yield, as a portion of the oil and its derivatives (e.g., LCFAs) adsorbed and encapsulated Na^+, thereby mitigating the inhibitory effects of LCFAs on microbes. Adding 8 g/L of oil with 9 g/L of NaCl also promoted living cell activity and ETS performance compared to the conditions with high oil or high salt alone. Microbial community analysis revealed that the co-occurrence of oil and salt promoted the enrichment of hydrolytic and acidogenic bacteria (e.g. Bacteroidetes, Proteobacteria, Thermotogae, and Synergistetes) and hydrogenotrophic methanogens (e.g., *Methanolinea*), with a concurrent upregulation of genes related to the hydrogenotrophic methanogenesis pathway (M00567).

CRediT authorship contribution statement

Han Shuang: Investigation, Formal analysis. **Ansari Ashley J.:** Writing – original draft, Methodology, Investigation. **Song Xiaoye:** Writing – review & editing, Validation, Supervision, Methodology, Funding acquisition, Conceptualization. **Peng Yongzhen:** Validation, Supervision. **Chen Xueqi:** Writing – original draft, Methodology, Investigation, Formal analysis.

Declaration of Competing Interest

The authors declare that they have no known competing financial interests or personal relationships that could have appeared to influence the work reported in this paper.

Acknowledgments

This research was supported by the National Natural Science Foundation of China (52300024).

Appendix A. Supporting information

Supplementary data associated with this article can be found in the online version at doi:10.1016/j.eti.2025.104208.

Data availability

Data will be made available on request.

References

Anwar, N., Wang, W., Zhang, J., Li, Y., Chen, C., Liu, G., Zhang, R., 2016. Effect of sodium salt on anaerobic digestion of kitchen waste. Water Sci. Technol. 73 (8), 1865–1871. https://doi.org/10.2166/wst.2016.035.

Benito, V., Etxebarria, J., Goñi-de-Cerio, F., Gonzalez, I., Brettes, P., Urkiaga, A., 2020. Better understanding of the activated sludge process combining fluorescence-based methods and flow cytometry: A case study. J. Environ. Sci. 90, 51–58. https://doi.org/10.1016/j.jes.2019.11.012.

Brown, M.R., Camézuli, S., Davenport, R.J., Petelenz-Kurdziel, E., Øvreås, L., Curtis, T.P., 2015. Flow cytometric quantification of viruses in activated sludge. Water Res 68, 414–422. https://doi.org/10.1016/j.watres.2014.10.018.

Buenaño-Vargas, C., Gagliano, M.C., Paulo, L.M., Bartle, A., Graham, A., van Veelen, H.P.J., O'Flaherty, V., 2024. Acclimation of microbial communities to low and moderate salinities in anaerobic digestion. Sci. Total Environ. 906, 167470. https://doi.org/10.1016/j.scitotenv.2023.167470.

Cai, C., Li, L., Hua, Y., Liu, H., Dai, X., 2021. Ferroferric oxide promotes metabolism in Anaerolineae other than microbial syntrophy in anaerobic methanogenesis of antibiotic fermentation residue. Sci. Total Environ. 758, 143601. https://doi.org/10.1016/j.scitotenv.2020.143601.

Cao, L., Cox, C.D., He, Q., 2021. Patterns of syntrophic interactions in methanogenic conversion of propionate. Appl. Microbiol. Biotechnol. 105 (23), 8937–8949. https://doi.org/10.1007/s00253-021-11645-9.

Chen, L., Hu, Q., Zhang, X., Chen, Z., Wang, Y., Liu, S., 2019. Effects of salinity on the biological performance of anaerobic membrane bioreactor. J. Environ. Manag. 238, 263–273. https://doi.org/10.1016/j.jenvman.2019.03.012.

Chen, X., Cui, Z., Zhao, Y., Zhu, N., Liu, Y., Hu, Z., Yuan, X., 2024. Synergistic mechanism of substrate hydrolysis and methanogenesis under "gradient anaerobic digestion" process. Energy Conv. Manag 309. https://doi.org/10.1016/j.enconman.2024.118443.

Chen, Y., Cheng, J.J., Creamer, K.S., 2008. Inhibition of anaerobic digestion process: a review. Bioresour. Technol. 99 (10), 4044–4064. https://doi.org/10.1016/j.biortech.2007.01.057.

Chung, M.M.S., Bao, Y., Domingo, J.A.V., Huang, J., 2023. Enhancing cleaning of microfiltration membranes fouled by food oily wastewater using microbubbles. Food Bioprod. Process 138, 53–59. https://doi.org/10.1016/j.fbp.2023.01.003.

Dang, Q., Zhao, X., Li, Y., Xi, B., 2023. Revisiting the biological pathway for methanogenesis in landfill from metagenomic perspective—A case study of county-level sanitary landfill of domestic waste in North China plain. Environ. Res. 222, 115185. https://doi.org/10.1016/j.envres.2022.115185.

De Temmerman, L., Maere, T., Temmink, H., Zwijnenburg, A., Nopens, I., 2014. Salt stress in a membrane bioreactor: Dynamics of sludge properties, membrane fouling and remediation through powdered activated carbon dosing. Water Res 63, 112–124. https://doi.org/10.1016/j.watres.2014.06.017.

Deaver, J.A., Soni, M.N., Diviesti, K.I., Finneran, K.T., Shankar, V., Popat, S.C., 2021. Taxonomic and Functional Variations Induced by an Overloading Event in Anaerobic Codigestion of Municipal Wastewater Sludge with Fats, Oils, and Grease. Acs EsT. Eng. 1 (8), 1205–1216. https://doi.org/10.1021/acsestengg.1c00086.

Dereli, R.K., van der Zee, F.P., Heffernan, B., Grelot, A., van Lier, J.B., 2014. Effect of sludge retention time on the biological performance of anaerobic membrane bioreactors treating corn-to-ethanol thin stillage with high lipid content. Water Res 49, 453–464. https://doi.org/10.1016/j.watres.2013.10.035.

Dereli, R.K., Heffernan, B., Grelot, A., van der Zee, F.P., van Lier, J.B., 2015. Influence of high lipid containing wastewater on filtration performance and fouling in AnMBRs operated at different solids retention times. Sep. Purif. Technol. 139, 43–52. https://doi.org/10.1016/j.seppur.2014.10.029.

Elsamadony, M., Mostafa, A., Fujii, M., Tawfik, A., Pant, D., 2021. Advances towards understanding long chain fatty acids-induced inhibition and overcoming strategies for efficient anaerobic digestion process. Water Res 190, 116732. https://doi.org/10.1016/j.watres.2020.116732.

Evans, P.N., Boyd, J.A., Leu, A.O., Woodcroft, B.J., Parks, D.H., Hugenholtz, P., Tyson, G.W., 2019. An evolving view of methane metabolism in the Archaea. Nat. Rev. Microbiol 17 (4), 219–232. https://doi.org/10.1038/s41579-018-0136-7.

Fujihira, T., Seo, S., Yamaguchi, T., Hatamoto, M., Tanikawa, D., 2018. High-rate anaerobic treatment system for solid/lipid-rich wastewater using anaerobic baffled reactor with scum recovery. Bioresour. Technol. 263, 145–152. https://doi.org/10.1016/j.biortech.2018.04.091.

Gao, Q., Zhao, Q., Wang, K., Li, X., Zhou, H., Ding, J., Li, L., 2024. Promoting methane production during anaerobic digestion with biochar: Is it influenced by quorum sensing? Chem. Eng. J. 483, 149268. https://doi.org/10.1016/j.cej.2024.149268.

García Rea, V.S., Muñoz Sierra, J.D., El-Kalliny, A.S., Cerqueda-García, D., Lindeboom, R.E.F., Spanjers, H., van Lier, J.B., 2023. Syntrophic acetate oxidation having a key role in thermophilic phenol conversion in anaerobic membrane bioreactor under saline conditions. Chem. Eng. J. 455, 140305. https://doi.org/10.1016/j.cej.2022.140305.

Gu, S., Xing, H., Zhang, L., Wang, R., Kuang, R., Li, Y., 2024. Effects of food wastes based on different components on digestibility and energy recovery in hydrogen and methane co-production. Heliyon 10 (3), e25421. https://doi.org/10.1016/j.heliyon.2024.e25421.

Han, S., Ansari, A.J., Zhang, N., Wu, C., Chen, X., Peng, Y., Song, X., 2024. Role of biochar addition to improve anaerobic membrane bioreactors to resist oil stress in synthetic food wastewater treatment. Environ. Technol. Innov. 35, 103665. https://doi.org/10.1016/j.eti.2024.103665.

He, J., Xia, S., Li, W., Deng, J., Lin, Q., Zhang, L., 2023. Resource recovery and valorization of food wastewater for sustainable development: An overview of current approaches. J. Environ. Manag. 347, 119118. https://doi.org/10.1016/j.jenvman.2023.119118.

He, Y.L., Xu, P., Li, C.J., Zhang, B., 2005. High-concentration food wastewater treatment by an anaerobic membrane bioreactor. Water Res 39 (17), 4110–4118. https://doi.org/10.1016/j.watres.2005.07.030.

Holohan, B.C., Duarte, M.S., Szabo-Corbacho, M.A., Cavaleiro, A.J., Salvador, A.F., Pereira, M.A., Ziels, R.M., Frijters, C.T.M.J., Pacheco-Ruiz, S., Carballa, M., Sousa, D.Z., Stams, A.J.M., O Flaherty, V., van Lier, J.B., Alves, M.M., 2022. Principles, Advances, and Perspectives of Anaerobic Digestion of Lipids. Environ. Sci. Technol. 56 (8), 4749–4775. https://doi.org/10.1021/acs.est.1c08722.

Hong, P., Noguchi, M., Matsuura, N., Honda, R., 2019. Mechanism of biofouling enhancement in a membrane bioreactor under constant trans-membrane pressure operation. J. Membr. Sci. 592, 117391. https://doi.org/10.1016/j.memsci.2019.117391.

Jang, H.M., Kim, J.H., Ha, J.H., Park, J.M., 2014. Bacterial and methanogenic archaeal communities during the single-stage anaerobic digestion of high-strength food wastewater. Bioresour. Technol. 165, 174–182. https://doi.org/10.1016/j.biortech.2014.02.028.

Jensen, P.D., Astals, S., Lu, Y., Devadas, M., Batstone, D.J., 2014. Anaerobic codigestion of sewage sludge and glycerol, focusing on process kinetics, microbial dynamics and sludge dewaterability. Water Res 67, 355–366. https://doi.org/10.1016/j.watres.2014.09.024.

Jeong, Y., Hermanowicz, S.W., Park, C., 2017. Treatment of food waste recycling wastewater using anaerobic ceramic membrane bioreactor for biogas production in mainstream treatment process of domestic wastewater. Water Res 123, 86–95. https://doi.org/10.1016/j.watres.2017.06.049.

Kumar Biswal, B., Huang, H., Dai, J., Chen, G., Wu, D., 2020. Impact of low-thermal pretreatment on physicochemical properties of saline waste activated sludge, hydrolysis of organics and methane yield in anaerobic digestion. Bioresour. Technol. 297, 122423. https://doi.org/10.1016/j.biortech.2019.122423.

Kurian, R., Acharya, C., Nakhla, G., Bassi, A., 2005. Conventional and thermophilic aerobic treatability of high strength oily pet food wastewater using membrane-coupled bioreactors. Water Res 39 (18), 4299–4308. https://doi.org/10.1016/j.watres.2005.08.030.

Lalman, J.A., Bagley, D.M., 2001. Anaerobic degradation and methanogenic inhibitory effects of oleic and stearic acids. Water Res 35 (12), 2975–2983. https://doi.org/10.1016/S0043-1354(00)00593-5.

Lei, Z., Wang, J., Leng, L., Yang, S., Dzakpasu, M., Li, Q., Li, Y., Wang, X.C., Chen, R., 2021. New insight into the membrane fouling of anaerobic membrane bioreactors treating sewage: Physicochemical and biological characterization of cake and gel layers. J. Membr. Sci. 632. https://doi.org/10.1016/j.memsci.2021.119383.

Li, J., Jiang, J., Li, J., He, C., Luo, Y., Wei, L., 2023. Anaerobic membrane bioreactors for wastewater treatment: mechanisms, fouling control, novel configurations, and future perspectives. Environ. Eng. Res. 28 (1), 210575. https://doi.org/10.4491/eer.2021.575.

Li, Q., Li, H., Wang, G., Wang, X., 2017. Effects of loading rate and temperature on anaerobic co-digestion of food waste and waste activated sludge in a high frequency feeding system, looking in particular at stability and efficiency. Bioresour. Technol. 237, 231–239. https://doi.org/10.1016/j.biortech.2017.02.045.

Li, S., Yuan, R., Chen, L., Wang, L., Hao, X., Wang, L., Zheng, X., Du, H., 2015. Systematic qualitative and quantitative assessment of fatty acids in the seeds of 60 tree peony (Paeonia section Moutan DC.) cultivars by GC–MS. Food Chem. 173, 133–140. https://doi.org/10.1016/j.foodchem.2014.10.017.

Li, Y., Zhang, S., Chen, Z., Ye, Z., Lyu, R., 2023. Multi-omics analysis unravels effects of salt and oil on substance transformation, microbial community, and transcriptional activity in food waste anaerobic digestion. Bioresour. Technol. 387, 129684. https://doi.org/10.1016/j.biortech.2023.129684.

Lin, H.J., Xie, K., Mahendran, B., Bagley, D.M., Leung, K.T., Liss, S.N., Liao, B.Q., 2009. Sludge properties and their effects on membrane fouling in submerged anaerobic membrane bioreactors (SAnMBRs). Water Res 43 (15), 3827–3837. https://doi.org/10.1016/j.watres.2009.05.025.

Liu, A., Dai, K., Wang, F., Yan, Y., Fu, D., 2024. Performance of anaerobic dynamic membrane bioreactor treatment of wastewater from food waste pretreatment: Dissolved organic matter changes and overloading effects. Environ. Technol. Innov. 35. https://doi.org/10.1016/j.eti.2024.103737.

Liu, N., Jiang, J., 2020. Valorisation of food waste using salt to alleviate inhibition by animal fats and vegetable oils during anaerobic digestion. Biomass-.-. Bioenergy 143, 105826. https://doi.org/10.1016/j.biombioe.2020.105826.

Liu, N., Wang, Q., Jiang, J., Zhang, H., 2017. Effects of salt and oil concentrations on volatile fatty acid generation in food waste fermentation. Renew. Energy 113, 1523–1528. https://doi.org/10.1016/j.renene.2017.07.042.

Liu, W., Song, X., Huda, N., Xie, M., Li, G., Luo, W., 2020. Comparison between aerobic and anaerobic membrane bioreactors for trace organic contaminant removal in wastewater treatment. Environ. Technol. Innov. 17, 100564. https://doi.org/10.1016/j.eti.2019.100564.

Liu, W., Xia, R., Ding, X., Cui, W., Li, T., Li, G., Luo, W., 2022. Impacts of nano-zero-valent iron on antibiotic removal by anaerobic membrane bioreactor for swine wastewater treatment. J. Membr. Sci. 659, 120762. https://doi.org/10.1016/j.memsci.2022.120762.

Long, J.H., Aziz, T.N., Reyes, F.L.D.L., Ducoste, J.J., 2012. Anaerobic co-digestion of fat, oil, and grease (FOG): A review of gas production and process limitations. Process Saf. Environ. Prot. 90 (3), 231–245. https://doi.org/10.1016/j.psep.2011.10.001.

Luo, J., Li, Y., Li, Y., Li, H., Fang, X., Li, Y., Huang, W., Cao, J., Wu, Y., 2021. Waste-to-energy: Cellulase induced waste activated sludge and paper waste co-fermentation for efficient volatile fatty acids production and underlying mechanisms. Bioresour. Technol. 341, 125771. https://doi.org/10.1016/j.biortech.2021.125771.

Ma, G., Chen, Y., Ndegwa, P., 2021. Association between methane yield and microbiota abundance in the anaerobic digestion process: A meta-regression. Renew. Sust. Energ. Rev. 135. https://doi.org/10.1016/j.rser.2020.110212.

Martinez-Quintela, M., Casas, G., Carramal, M., Vega, E., Llenas, L., Paredes, L., 2024. Valorizing meat processing industry brines to produce added-value organic acids. J. Environ. Manag. 371, 122982. https://doi.org/10.1016/j.jenvman.2024.122982.

Meng, F., He, X., 2015. Effects of naturally occurring grit on the reactor performance and microbial community structure of membrane bioreactors. J. Membr. Sci. 496, 284–292. https://doi.org/10.1016/j.memsci.2015.09.015.

Miao, L., Zhang, Q., Wang, S., Li, B., Wang, Z., Zhang, S., Zhang, M., Peng, Y., 2018. Characterization of EPS compositions and microbial community in an Anammox SBBR system treating landfill leachate. Bioresour. Technol. 249, 108–116. https://doi.org/10.1016/j.biortech.2017.09.151.

Ninomiya, Y., Kimura, K., Sato, T., Kakuda, T., Kaneda, M., Hafuka, A., Tsuchiya, T., 2020. High-flux operation of MBRs with ceramic flat-sheet membranes made possible by intensive membrane cleaning: Tests with real domestic wastewater under low-temperature conditions. Water Res 181, 115881. https://doi.org/10.1016/j.watres.2020.115881.

Niu, Z., Guo, H., Zhou, Y., Xia, S., 2021. Unraveling membrane fouling in anoxic/oxic membrane bioreactors treating anaerobically digested piggery wastewater. J. Environ. Chem. Eng. 9 (1), 104985. https://doi.org/10.1016/j.jece.2020.104985.

Okoro, C., Ekun, O.A., Nwume, M.I., Lin, J., 2016. Molecular analysis of microbial community structures in Nigerian oil production and processing facilities in order to access souring corrosion and methanogenesis. Corros. Sci. 103, 242–254. https://doi.org/10.1016/j.corsci.2015.11.024.

Palatsi, J., Affes, R., Fernandez, B., Pereira, M.A., Alves, M.M., Flotats, X., 2012. Influence of adsorption and anaerobic granular sludge characteristics on long chain fatty acids inhibition process. Water Res 46 (16), 5268–5278. https://doi.org/10.1016/j.watres.2012.07.008.

Putra, A.A., Watari, T., Maki, S., Hatamoto, M., Yamaguchi, T., 2020. Anaerobic baffled reactor to treat fishmeal wastewater with high organic content. Environ. Technol. Innov. 17. https://doi.org/10.1016/j.eti.2019.100586.

Ramos, C., García, A., Diez, V., 2014. Performance of an AnMBR pilot plant treating high-strength lipid wastewater: Biological and filtration processes. Water Res 67, 203–215. https://doi.org/10.1016/j.watres.2014.09.021.

Rasit, N., Idris, A., Harun, R., Wan Ab Karim Ghani, W.A., 2015. Effects of lipid inhibition on biogas production of anaerobic digestion from oily effluents and sludges: An overview. Renew. Sustain. Energy Rev. 45, 351–358. https://doi.org/10.1016/j.rser.2015.01.066.

Sorokin, D.Y., Chernyh, N.A., 2016. Candidatus Desulfonatronobulbus propionicus': a first haloalkaliphilic member of the order Syntrophobacterales from soda lakes. Extremophiles 20 (6), 895–901. https://doi.org/10.1007/s00792-016-0881-3.

Sun, M., Zhang, C., Shi, Z., Zhang, C., Zhang, S., Luo, G., 2023. Genome-centric metagenomic analysis revealed the microbial shifts in response to long-chain fatty acids (LCFA) in anaerobic digestion with hydrochar. Chem. Eng. J. 466, 143249. https://doi.org/10.1016/j.cej.2023.143249.

Szabo-Corbacho, M.A., Sharma, P., Míguez, D., de la Sovera, V., Brdjanovic, D., Etchebehere, C., García, H.A., van Lier, J.B., 2024. Inhibitory effects of long chain fatty acids on anaerobic sludge treatment: Biomass adaptation and microbial community assessment. Environ. Technol. Innov. 33, 103529. https://doi.org/10.1016/j.eti.2024.103529.

Tian, T., Qiao, S., Yu, C., Tian, Y., Yang, Y., Zhou, J., 2017. Distinct and diverse anaerobic respiration of methanogenic community in response to MnO2 nanoparticles in anaerobic digester sludge. Water Res 123, 206–215. https://doi.org/10.1016/j.watres.2017.06.066.

Wang, K., Zhang, H., Shen, Y., Li, J., Zhou, W., Song, H., Liu, M., Wang, H., 2023. Impact of salinity on anaerobic ceramic membrane bioreactor for textile wastewater treatment: Process performance, membrane fouling and machine learning models. J. Environ. Manag. 345, 118717. https://doi.org/10.1016/j.jenvman.2023.118717.

Wang, L., Wu, Y., Fu, Y., Deng, L., Wang, Y., Ren, Y., Zhang, H., 2022. Low electric field assisted surface conductive membrane in AnMBR: Strengthening effect and fouling behavior. Chem. Eng. J. 431, 133185. https://doi.org/10.1016/j.cej.2021.133185.

Wang, P., Li, X., Li, Y., Su, Y., Wu, D., Xie, B., 2023. Enhanced anaerobic digestion performance of food waste by zero-valent iron and iron oxides nanoparticles: Comparative analyses of microbial community and metabolism. Bioresour. Technol. 371. https://doi.org/10.1016/j.biortech.2023.128633.

Wu, Q.L., Guo, W.Q., Bao, X., Zheng, H.S., Yin, R.L., Feng, X.C., Luo, H.C., Ren, N.Q., 2017. Enhanced volatile fatty acid production from excess sludge by combined free nitrous acid and rhamnolipid treatment. Bioresour. Technol. 224, 727–732. https://doi.org/10.1016/j.biortech.2016.10.086.

Wu, Y., Hu, W., Zhu, Z., Zheng, X., Chen, Y., Chen, Y., 2023. Enhanced Volatile Fatty Acid Production from Food Waste Fermentation via Enzymatic Pretreatment: New Insights into the Depolymerization and Microbial Traits. Acs EsT. Eng. 3 (1), 26–35. https://doi.org/10.1021/acsestengg.2c00219.

Xiao, K., Maspolim, Y., Zhou, Y., Guo, C., Ng, W.J., 2022. Effect of Sodium on Methanogens in a Two-Stage Anaerobic System. Appl. Sci. 12 (3), 956. https://doi.org/10.3390/app12030956.

Xiao, X., Shi, W., Huang, Z., Ruan, W., Miao, H., Ren, H., Zhao, M., 2017. Process stability and microbial response of anaerobic membrane bioreactor treating high-strength kitchen waste slurry under different organic loading rates. Int. Biodeterior. Biodegrad 121, 35–43. https://doi.org/10.1016/j.ibiod.2017.03.012.

Xu, R., Fang, S., Zhang, L., Huang, W., Shao, Q., Fang, F., Feng, Q., Cao, J., Luo, J., 2021. Distribution patterns of functional microbial community in anaerobic digesters under different operational circumstances: A review. Bioresour. Technol. 341, 125823. https://doi.org/10.1016/j.biortech.2021.125823.

Yin, Q., Miao, J., Li, B., Wu, G., 2017. Enhancing electron transfer by ferroferric oxide during the anaerobic treatment of synthetic wastewater with mixed organic carbon. Int. Biodeterior. Biodegrad 119, 104–110. https://doi.org/10.1016/j.ibiod.2016.09.023.

Yun, H., Liang, B., He, Z., Li, M., Zong, S., Wang, Z., Ge, B., Zhang, P., Li, X., Wang, A., 2023. Insights into methanogenesis of mesophilic-psychrophilic varied anaerobic digestion of municipal sludge with antibiotic stress. J. Environ. Manag. 331, 117278. https://doi.org/10.1016/j.jenvman.2023.117278.

Zhang, H., Zhao, J., Fu, Z., Wang, Y., Guan, D., Xie, J., Zhang, Q., Liu, Q., Wang, D., Sun, Y., 2023. Metagenomic approach reveals the mechanism of calcium oxide improving kitchen waste dry anaerobic digestion. Bioresour. Technol. 387, 129647. https://doi.org/10.1016/j.biortech.2023.129647.

Zhao, J., Zhang, C., Wang, D., Li, X., An, H., Xie, T., Chen, F., Xu, Q., Sun, Y., Zeng, G., Yang, Q., 2016. Revealing the Underlying Mechanisms of How Sodium Chloride Affects Short-Chain Fatty Acid Production from the Cofermentation of Waste Activated Sludge and Food Waste. Acs Sustain. Chem. Eng. 4 (9), 4675–4684. https://doi.org/10.1021/acssuschemeng.6b00816.

Zhao, J., Liu, Y., Wang, D., Chen, F., Li, X., Zeng, G., Yang, Q., 2017. Potential impact of salinity on methane production from food waste anaerobic digestion. Waste Manag. 67, 308–314. https://doi.org/10.1016/j.wasman.2017.05.016.